

# Biochemical and EPR-Spectroscopic Investigation into Heterologously Expressed Vinyl Chloride Reductive Dehalogenase (VcrA) from *Dehalococcoides mccartyi* Strain VS

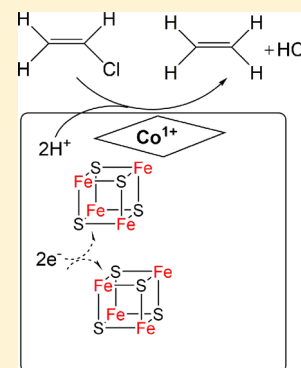
Anutthaman Parthasarathy,<sup>†</sup> Troy A. Stich,<sup>‡</sup> Svenja T. Lohner,<sup>†</sup> Ann Lesnefsky,<sup>†</sup> R. David Britt,<sup>‡</sup> and Alfred M. Spormann<sup>\*,†</sup>

<sup>†</sup>Departments of Chemical Engineering and Civil and Environmental Engineering, Stanford University, Stanford, California 94305, United States

<sup>‡</sup>Department of Chemistry, University of California, Davis, Davis, California 95616, United States

## Supporting Information

**ABSTRACT:** Reductive dehalogenases play a critical role in the microbial detoxification of aquifers contaminated with chloroethenes and chloroethanes by catalyzing the reductive elimination of a halogen. We report here the first heterologous production of vinyl chloride reductase VcrA from *Dehalococcoides mccartyi* strain VS. Heterologously expressed VcrA was reconstituted to its active form by addition of hydroxocobalamin/adenosylcobalamin, Fe<sup>3+</sup>, and sulfide in the presence of mercaptoethanol. The kinetic properties of reconstituted VcrA catalyzing vinyl chloride reduction with Ti(III)-citrate as reductant and methyl viologen as mediator were similar to those obtained previously for VcrA as isolated from *D. mccartyi* strain VS. VcrA was also found to catalyze a novel reaction, the environmentally important dihaloelimination of 1,2-dichloroethane to ethene. Electron paramagnetic resonance (EPR) spectroscopic studies with reconstituted VcrA in the presence of mercaptoethanol revealed the presence of Cob(II)alamin. Addition of Ti(III)-citrate resulted in the appearance of a new signal characteristic of a reduced [4Fe-4S] cluster and the disappearance of the Cob(II)alamin signal. UV-vis absorption spectroscopy of Ti(III) citrate-treated samples revealed the formation of two new absorption maxima characteristic of Cob(I)alamin. No evidence for the presence of a [3Fe-4S] cluster was found. We postulate that during the reaction cycle of VcrA, a reduced [4Fe-4S] cluster reduces Co(II) to Co(I) of the enzyme-bound cobalamin. Vinyl chloride reduction to ethene would be initiated when Cob(I)alamin transfers an electron to the substrate, generating a vinyl radical as a potential reaction intermediate.



## INTRODUCTION

Chloroethenes, such as tetrachloroethene (PCE), trichloroethene (TCE), the dichloroethenes (DCE), vinyl chloride (VC), as well as the chloroethanes 1,1,2-trichloroethane (TCA), and 1,2-dichloroethane (DCA), are the most prevalent groundwater contaminants in developed countries including the United States.<sup>1-3</sup> Key for the microbial degradation of such chlorinated aliphatic hydrocarbons to harmless organic compounds are catabolic reductive dehalogenases (Rdh). Rdh's are highly oxygen-sensitive enzymes and catalyze the reductive elimination of a halide. The catalytically active subunit RdhA contains a corrinoid and two [4Fe-4S] clusters and is typically associated with the outer leaflet of the cytoplasmic membrane presumably via the small integral membrane protein RdhB. Rdh's are unique among the FeS cluster/corrinoid enzymes in that they catalyze a net reduction reaction directly by the cobalamin without the intervention of other organic cofactor radicals.<sup>4</sup>

Current understanding of Rdh is limited to results from studies with only a few purified enzymes, PceA,<sup>5,6</sup> CprA,<sup>7,8</sup> TceA,<sup>9</sup> and VcrA.<sup>10</sup> These studies indicated a relatively high degree of substrate specificity of each Rdh. More recently, dihaloeliminating reductive dehalogenases were identified, resulting in the

formation of chloroethenes from chloroethanes.<sup>11,12</sup> Thus, the degradations of both classes of organohalogenes intersect via a mosaic metabolic network of diverse Rdh's.<sup>11</sup> Whether such dihaloeliminating activities are due to a single, mono-, and dihaloeliminating Rdh or the concerted action of two specific Rdh's has not been revealed. However, dihaloelimination is of critical importance for successfully engineering bioremediation and avoiding accumulation of more toxic intermediates such as vinyl chloride.

Reductive dehalogenation is a catabolic process coupling energy conservation with a dehalogenation reaction. It is found primarily in the anaerobic *Dehalococcoides*-, *Sulfurospirillum*-, and *Dehalobacter*-type microorganisms. In *Dehalobacter restrictus*,<sup>13</sup> *Desulfomonile tiedjei*,<sup>14</sup> and *Sulfurospirillum multivorans*,<sup>15</sup> reductive dehalogenation is one of many possible modes of energy conservation. In contrast, *Dehalococcoides* sp. are highly niche-specialized and can only conserve energy by reductive dehalogenation. *Dehalococcoides* Rdh's are unique and distinctive in that the electrons for chloroethene reduction are derived

Received: November 19, 2014

Published: February 16, 2015

obligatorily from H<sub>2</sub>. Hydrogen is presumably oxidized by a HupL hydrogenase, which appears to form a membrane-bound complex facing the outside of the cell with an Rdh (Supporting Information Figure S1).<sup>16</sup> How the electrons are transferred to an Rdh, and how *Dehalococcoides* spp. conserve metabolic energy during this unique respiratory process, are unknown.

The development of a molecular understanding of *Dehalococcoides*-type Rdh's, in particular the study of the reaction mechanism, has been hampered by the slow doubling time of the microorganisms, the low biomass yield, and the oxygen sensitivity of native Rdh's. Numerous unsuccessful attempts have been conducted by different research groups to heterologously produce active Rdh's. Only recently were two reductive dehalogenases heterologously expressed in the background of a dehalogenating strain: reductive dehalogenase (PceA) of *Desulfitobacterium hafniense* strain Y51 was overexpressed in *Shimwellia blattae*<sup>17</sup> and the NpRdhA of *Nitratireductor pacificus* in *Bacillus megaterium*.<sup>18</sup> We report here the first successful heterologous overproduction in *E. coli* of a *Dehalococcoides*-type Rdh, its reconstitution to an active form, as well as its initial biochemical characterization.

## EXPERIMENTAL SECTION

**Plasmid Construction.** Standard protocols<sup>19</sup> were used for all genetic work. Promega kits were used for isolation and purification of DNA. Vector pLIC-HMK (a gift from Dr. James Berger, University of California, Berkeley) was used as the plasmid backbone. The *vcrA* gene (vinyl chloride reductase A) from *Dehalococcoides* VS (NCBI Gene ID: 8658217, NC\_013552.1:complement(1187299–1188753)) devoid of the first 35 amino acids of the 5' region coding for the TAT-signal peptide was amplified from the genomic DNA of *Dehalococcoides mccartyi* strain VS using 5'-TAC TTC CAA TCC AAT GCA GACATTGATGAACCTTGTTC AAGC-3' as the upstream primer and 5'-T TAT TCA CTT CCA ATG TTA TTA AGTACCGGATCAAAGCC-3' as the downstream primer, and inserted into pLIC-HMK using ligation independent cloning or LIC<sup>20</sup> to create an IPTG inducible N-terminal, 6x-Histidine, Maltose Binding Protein (MBP), TEV protease cleavage site *vcrA* fusion gene.<sup>21,22</sup> Fermentas LIC qualified T4 DNA polymerase was used to perform the LIC reaction. The fidelity of the entire gene fusion was verified by DNA sequencing. This plasmid was denoted NNHM-VcrA for N-terminus, no TAT signal sequence, 6x-histidine tag, maltose binding protein *vcrA* gene fusion. For simplicity, we address the NNHM-VcrA protein in this Article as VcrA-MBP with the understanding that it is the fusion protein, as described here: refer to Supporting Information Figure S2.

**Heterologous Expression of VcrA-MBP in *E. coli*.** pLIC-HMK NNHM-VcrA was transformed into chemically competent cells of *E. coli* BL21 DE3. Five milliliter cultures of this strain were grown overnight at 37 °C in noninducing minimal medium (MDG medium<sup>23</sup>) supplemented with 2 g/L glucose and 100 µg/mL of kanamycin. The overnight cultures were then inoculated into LB medium supplemented with 0.2% (w/v) of glucose and 100 µg/mL of Kanamycin up to an initial OD<sub>600</sub> of 0.1. After the cultures had reached an OD<sub>600</sub> of 0.5 at 37 °C, expression of the plasmid was induced upon addition of 1 mM IPTG final concentration. Following 3 h of induction, the cells were harvested by centrifugation at 6000g at 4 °C for 20 min on a Beckman Coulter Avanti J-20 XP centrifuge. The overproduction was verified by SDS PAGE. The bulk of the overproduced protein was found in the insoluble fraction (data not shown).

**Purification of VcrA-MBP by Affinity Chromatography.** Three grams of Ni-IDA or Ni-TED bonded to silica<sup>24,25</sup> for His-Tag affinity chromatography (Protino Ni-IDA Resin & Protino Ni-TED Resin, Macherey Nagel) was added as a slurry in distilled water to a 20 mL fritted column (diameter 2 cm) and allowed to pack by gravity to about 8 mL volume. Gentle suction was applied at the bottom of the column through a vacuum line to drain the aqueous phase. Dry columns were stored at room temperature until use.

All subsequent operations were carried out in a Coy anoxic chamber (95% N<sub>2</sub>, 5% H<sub>2</sub>). All buffers, filters, centrifuge tubes, and columns were incubated at least overnight in the anoxic chamber prior to use. Buffers and solutions were filtered through a sintered glass filter layered with Whatman GF/C 55 mm glass fiber filters and were subsequently subjected to 4 cycles of degassing and purging with nitrogen (99.99%). In the anoxic chamber, 2 mM 2-mercaptoethanol final concentration was added to all solutions and buffers.

About 3 g wet weight of induced cells carrying pLIC-HMK NNHM-VcrA was resuspended in ca. 30 mL of buffer A (50 mM potassium phosphate pH 8.0 containing 0.5 M NaCl, 20% (v/v) glycerol, and 1 mM PMSF as a protease inhibitor). After sonication in the anoxic chamber at 70% power for 15 min (30 s pulse followed by 30 s cooling) at 4 °C, the suspension was centrifuged for 30 min at 4 °C at 30 000g on a Beckman Coulter Avanti J-20 XP centrifuge. The supernatant was discarded and the pellet resuspended in 15 mL of denaturing buffer (Buffer A + 8 M urea). Following another round of sonication at 70% power for 15 min (30 s pulse followed by 30 s cooling) at 4 °C, the suspension was stirred on ice for 60 min to solubilize the pellet. Another centrifugation for 30 min at 4 °C at 10 000g was performed to remove any remaining insoluble material.

The supernatant containing denatured VcrA-MBP was loaded onto the Ni-IDA column, which had been washed with 5 column volumes of buffer A and equilibrated with 3 column volumes of denaturing buffer. VcrA-MBP elution was achieved with 3 column volumes of 250 mM imidazole in the denaturing buffer. The eluted fractions were collected and analyzed separately. The samples were desalted with PD-10 columns (GE Healthcare), which had been previously washed with several volumes of anoxic buffer, to remove urea and imidazole, and eluted with buffer A containing 0.2% CHAPS (3-[(3-cholamidopropyl)-dimethylammonio]-1-propanesulfonate) as detergent. The eluted fractions were pooled and allowed to refold in the refolding buffer (50 mM Tris pH 8.0 containing 0.5 M NaCl, 20% (v/v) glycerol, 0.2% CHAPS, and 1 mM PMSF (phenylmethylsulfonyl fluoride) as a protease inhibitor and 2 mM 2-mercaptoethanol) for 1 h at room temperature and then concentrated via Amicon Ultracel 50 K centrifugal filters (EMD Millipore) at 6000g on a Clay Adams Compact II centrifuge. The concentrated protein was mixed with a minimum volume of the refolding buffer and frozen at -80 °C until further use. The purity of VcrA-MBP was verified by SDS-PAGE (Figure 1) and peptide mass fingerprinting of the corresponding SDS gel band.

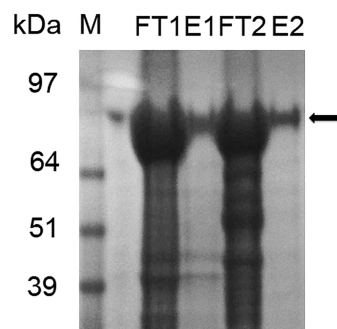


**Figure 1.** SDS-PAGE of VcrA-MBP purified by Ni-TED and Ni-IDA His-tag affinity chromatography columns under denaturing conditions. The arrow indicates the band corresponding to purified VcrA-MBP. M is the molecular mass marker. FT = flow through from the column and E = elution with 250 mM imidazole. Sample 1 was processed with a Ni-TED column and sample 2 with a Ni-IDA column.

**Cofactor Reconstitution.** Anoxic solutions of 200 mM DTT, 100 mM FeCl<sub>3</sub>, and 30 mM Na<sub>2</sub>S·9H<sub>2</sub>O were prepared in degassed 100 mM Tris-HCl pH 7.4 purged with 99.99% N<sub>2</sub> prior to the cofactor reconstitution. To initiate the reconstitution of the iron-sulfur clusters of VcrA or VcrA-MBP, the protein was reduced by the addition of 5 mM DTT, and the solution was incubated at room temperature for 30 min to be completely reduced. The iron-sulfur clusters were subsequently

reconstituted by adding  $\text{FeCl}_3$  at 5 mol excess over protein and  $\text{Na}_2\text{S}$  at 10 mol excess over protein to the mixture, which was then incubated at room temperature for 90 min. Precipitated protein and iron sulfide particles were removed by centrifugation at 5000g for 5 min. Finally, adenosyl- or hydroxocobalamin was added to a final concentration of 10 mg/mL, and the mixture was incubated at room temperature for 30 min. Unbound iron sulfide and cobalamin were removed by passage through PD-10 columns (GE Healthcare). The samples were filtered through 0.2  $\mu\text{m}$  Thermo Scientific Nalgene Syringe filters, eluted with the refolding buffer, concentrated to ca. 20 mg/mL, and stored at  $-80^\circ\text{C}$  until further use. The reconstitution of the enzyme could be performed with any one of the following  $\text{B}_{12}$  derivatives, adenosylcobalamin, hydroxocobalamin, dicyanocobinamide, or aquahydroxocobinamide, although only the first two were used for trials involving activity assays.

**TEV-Protease Digestion and Purification of Untagged VcrA.** Samples of purified but unassembled VcrA-MBP apoprotein were digested anaerobically with manufacturer-recommended amounts of Pro-TEV (Promega) protease (which contains a HQ tag allowing for His-tagged affinity chromatography) in 50 mM Tris HCl pH 8.0 free of protease inhibitors for 3 h at  $20^\circ\text{C}$  to remove the MBP and His tags. The digest was passed over a Ni-IDA column, which retained Pro-TEV protease via its HQ tag as well as the His-MBP tag of VcrA. The untagged VcrA (defined here and described as "VcrA" as opposed to the parent "VcrA-MBP") was collected from the flow through and confirmed pure by PAGE (Supporting Information Figure S3); 3 mg of VcrA-MBP yielded 0.8 mg of untagged VcrA.

**SDS-PAGE and Protein Determination.** Samples for SDS-PAGE and protein quantification were prepared by using Zeba Micro Spin desalting columns 7 MWCO (Thermo Scientific) following the manufacturer's protocol and eluted in distilled water. Further processing for SDS-PAGE was performed according to the NuPage Novex system (Invitrogen). NuPage Novex 1.0 mm BisTris 10–12% acrylamide precast gels (Invitrogen) were used for the PAGE analysis. The SeeBlue Plus2 Prestained Standard (Invitrogen) was used as a molecular weight marker. Protein concentrations were determined by the BCA assay using the Micro BCA Protein Assay Kit (Thermo Scientific), using Bovine Serum Albumin as standard.

**Metal Analysis.** For metal analysis, concentrated enzyme (either VcrA-MBP or VcrA) was desalted, eluted in distilled water, digested with 5% HCl, and filtered to remove the precipitated protein. Nonheme iron in the protein was quantified with Ferene (3-(2-pyridyl)-5,6-bis(5-sulfo-2-furyl)-1,2,4-triazine, disodium trihydrate).<sup>26,27</sup> For the calibration curve, 2–20  $\mu\text{M}$  standards were prepared freshly from a stock solution containing 0.2 mM  $(\text{NH}_4)_2\text{Fe}(\text{SO}_4)_2 \cdot 6\text{H}_2\text{O}$ . The iron standards, the water reference, and the protein-containing solutions were each filled with  $\text{H}_2\text{O}$  to a final volume of 100  $\mu\text{L}$ . The solutions were mixed with 100  $\mu\text{L}$  of 1% HCl (v/v) and incubated at  $80^\circ\text{C}$  for 10 min. After the solutions were cooled to room temperature, 500  $\mu\text{L}$  of ammonium acetate 7.5% (w/v), 100  $\mu\text{L}$  of ascorbic acid 4% (w/v), 100  $\mu\text{L}$  of SDS 2.5% (w/v), and 100  $\mu\text{L}$  of Ferene 1.5% (w/v) were sequentially added into each sample with vortex mixing. The Eppendorf tubes containing the reaction mixtures were centrifuged at 13 000g for 10 min. The supernatant was used for measuring the UV–vis absorbance at 593 nm. The iron content of the protein solution was calculated from the calibration curve of the absorbance.

Cobalt content was analyzed by ICP-MS.<sup>28,29</sup> Solutions of 5 mL were prepared for the cobalt standards, and samples of unknown concentration were prepared in clean unused plastic BD tubes in 5% HCl. The calibration curve was from 0.1 to 5000 parts per billion. The samples were analyzed on a Thermo XSeries II ICP-MS, with a 60 s rinse of 3% nitric acid between samples and an uptake time of 60 s for each sample. Three readings were collected, and the average was reported. Internal standards of cobalt (2.5 and 5 ppm) were used; scandium and yttrium were used for corrections.

**GC Methods.** Chloro-ethenes and ethanes were quantified by gas chromatography using an Agilent Technologies 6890 Network GC System instrument equipped with a flame ionization detector (FID) and an HP 624 Special Analysis column (capillary 30.0 m  $\times$  530  $\mu\text{m}$   $\times$  300  $\mu\text{m}$ ). The injector was maintained at  $200^\circ\text{C}$ , and the FID was operated at  $280^\circ\text{C}$ . Helium was used as carrier gas (99.9% purity) at a pressure of

4.86 psi and a flow rate of 5.1 mL/min. The temperature program was 8.6 min at  $100^\circ\text{C}$  with no ramping.

**VcrA Activity Assays.** All enzyme activity experiments were performed in triplicate in anoxic, sealed crimped serum vials of 10 mL volume stoppered with butyl rubber stoppers, containing 6 mL of the aqueous phase and 4 mL of headspace. 0.1 mL headspace samples were injected into the GC for analyses. Standards of ethene were prepared by diluting a commercial 1.01% standard (Supelco) into serum vials, assuming an ideal gas volume of 22.4 L per mole. For the chlorinated compounds, commercial standards of 2 mg/mL dissolved in methanol (Supelco) were diluted into the serum vials.

Henry's constants  $K_{\text{H}}^{\text{cc}}$  at  $20^\circ\text{C}$  from the US EPA Web site (<http://www.epa.gov/athens/learn2model/part-two/onsite/esthenry.html>) were used to calculate the partition of 1,1-DCE, VC, and 1,2-DCA between gas and aqueous phases. For ethene, a  $K_{\text{H}}^{\text{cc}}$  of 7.6 was used.<sup>30</sup> Calibration curves obtained by correlating peak area and the number of moles were used for calculation of the number of moles observed in the enzymatic assays.

A typical assay mixture in an anoxic 10 mL serum vial contained 0.2–1 mg/mL of fully reconstituted VcrA, with 1 mM Ti(III) citrate and 0.4 mM methyl viologen as electron donor and mediator, respectively, in 50 mM Tris-HCl pH 8.5. The reaction was started by injecting a defined volume of aqueous 1,1-DCE from a saturated aqueous solution of approximately 26 mM. For vinyl chloride, a methanolic solution of 32 mM was used; for 1,2-DCA, an aqueous stock solution of 100 mM was used. The incubation time was generally 60 min; the 1,1-DCE concentrations and the incubation times were varied during different experiments. For cobalamin-only measurements, the same mixture was used; enzyme was omitted and 2 mg/mL cobalamin was added. After allowing the reaction to proceed for a specified time, the reaction was stopped by the addition of 0.1 mL of concentrated HCl.

**Peptide Mass Fingerprinting (PMF).** Mass mapping was performed at the PAN Center, Stanford University, using a 4700 Proteomics Analyzer that features tandem (MS/MS) time-of-flight (TOF) optics to provide peptide structural information, in addition to high accuracy MS data. The data showed 25–60 ppm accuracy in mass mapping experiments without the need for internal calibration. The laser repetition rate was 200 Hz. Sample preparation for PMF was carried out as follows: 45 mM dithiothreitol (Sigma) in 10 mM ammonium bicarbonate (pH 7.8) was added to polyacrylamide gel slices and then incubated for 30 min at  $55^\circ\text{C}$ . The solution was changed to 100 mM acrylamide (Bio-Rad) in 10 mM ammonium bicarbonate and incubated 1 h at room temperature. The ammonium bicarbonate solution was removed, and 0.5 mL of 10 mM ammonium bicarbonate and 50% acetonitrile were added to the gel and incubated for 30 min. The gel slice was then dried to completion. A small volume (2–10  $\mu\text{L}$ ) of 10 mM ammonium bicarbonate containing 4–20 pmol of trypsin (Promega) was added to the slice. The gel was then saturated with 10 mM ammonium bicarbonate buffer. Buffer was added continuously over 2 h until the gel was swollen and covered with buffer. The gel was then incubated with trypsin overnight at  $37^\circ\text{C}$ .

Peptides were extracted onto Ziptips (Millipore) from an aliquot of the solution and then washed with 0.1% trifluoroacetic acid (Applied Biosystems) and eluted directly to a matrix-assisted laser desorption ionization (MALDI) plate with 0.5  $\mu\text{L}$  of 50% acetonitrile and 0.1% trifluoroacetic acid. The eluate was partially dried, and then 0.5  $\mu\text{L}$  of  $\alpha$ -cyano-4-hydrozycinnamic acid (Agilent) (5 mg/mL) was added. MALDI-mass spectrometry (MS) was performed using the reflector mode to obtain monoisotopic peptide masses and tandem MS. The results were then used to search protein and genomic databases with the Mascot software. Further details are given in Bechtel et al.<sup>31</sup>

**EPR Spectroscopy.** Samples for X-band EPR spectroscopy were prepared in 3.8 mm thin walled precision quartz EPR sample tubes (Wilmad Lab Glass) by freezing anaerobically prepared, buffered protein solutions with 20% (v/v) of 4 M sucrose as a glassing agent in liquid nitrogen and capping the tubes immediately. The frozen samples were stored in liquid nitrogen.

All EPR spectra were measured at the CalEPR Center at the University of California, Davis. Continuous-wave (CW) X-band spectra were acquired with an E-500 spectrometer (Bruker, Billerica, MA) under

Table 1. Substrates Tested in This Study for Transformation by VcrA and VcrA-MBP, and Their Michaelis–Menten Parameters<sup>a</sup>

substrate	VcrA-MBP (molar mass 100 kDa)					VcrA, no MBP (molar mass 57 kDa)				
	$V_{\max}$ [nmol min <sup>-1</sup> (mg protein) <sup>-1</sup> ] with MV	$K_{\text{cat}}$ [s <sup>-1</sup> ] with MV	$V_{\max}$ [nmol min <sup>-1</sup> (mg protein) <sup>-1</sup> ] without MV	$K_{\text{cat}}$ [s <sup>-1</sup> ] without MV	$K_M$ [ $\mu\text{M}$ ]	$V_{\max}$ [nmol min <sup>-1</sup> (mg protein) <sup>-1</sup> ] with MV	$K_{\text{cat}}$ [s <sup>-1</sup> ] with MV	$V_{\max}$ [nmol min <sup>-1</sup> (mg protein) <sup>-1</sup> ] without MV	$K_{\text{cat}}$ [s <sup>-1</sup> ] without MV	$K_M$ [ $\mu\text{M}$ ]
1,1-DCE	295	177	73	43.8	50	675	578	300	257	45
VC	1050	630	265	159	10	2250	1928	1006	862	13
1,2-DCA	450	270	80	96	1300	722	618	395	338	1300

<sup>a</sup>VcrA, enzyme without MBP and His tags; VcrA-MBP, enzyme with His and MBP tags intact; MV, methyl viologen.

nonsaturating slow-passage conditions using a Super-High Q resonator (ER 4122SHQE). Cryogenic temperatures were achieved and maintained using an Oxford Instruments ESR900 liquid helium cryostat in conjunction with an Oxford Instruments ITC503 temperature and gas-flow controller. Spectral simulations were performed with Matlab using the EasySpin 4.0 toolbox.<sup>32</sup> Quantitation of the concentration of  $S = 1/2$  spin systems in the vicinity of  $g = 2$  concentration within a sample was achieved by comparing the double integral of the EPR intensity to that of a 308  $\mu\text{M}$  Cu(II) in 100 mM EDTA (EDTA = ethylenediaminetetraacetic acid) at pH 7 spin-standard.<sup>33</sup> All data were corrected for differences in incident microwave power, acquisition temperature, and cavity quality factor. All concentrations are given in micromolar.

**Detection of Co(I) and Co(II) Cobalamins by Electronic Absorption Spectroscopy.** Enzyme-bound Cob(I)alamin was detected in VcrA-MBP by the UV–vis absorption at 385 nm (388 nm for VcrA) and 555 nm (550 nm for VcrA) and estimated by the measured extinction coefficients of 22  $\text{mM}^{-1} \text{cm}^{-1}$  at 385 or 388 nm and 9  $\text{mM}^{-1} \text{cm}^{-1}$  at 550 or 555 nm. For the detection of the enzyme-bound Cob(II)alamin, the absorbance at 475 nm was monitored ( $\epsilon = 9.47 \text{ mM}^{-1} \text{cm}^{-1}$  at 477 nm<sup>34</sup>). The spectra were measured on an Ultrospec 2100 Pro UV–visible spectrophotometer (Amersham Biosciences) in cuvettes of 1 cm path length.

**Synthesis and Purification of Aquahydroxocobinamide [(H<sub>2</sub>O)OHcbi].** Ten milligrams of (CN)<sub>2</sub>Cbi or dicyanocobinamide (Sigma-Aldrich), whose UV–visible spectrum was identical to the reported spectrum,<sup>35,36</sup> was dissolved in 3 mL of anaerobic 0.1 M NaOH, and small aliquots of sodium borohydride pellets were added every 5 min, until a molar excess of about 10-fold of borohydride over (CN)<sub>2</sub>Cbi was reached. The reaction proceeded for about 1.5 h until the mixture was transferred into a beaker and quenched by the addition of acidified water. The final pH was adjusted to 3, and the mixture was purified over a 1 g Sep Pak C<sub>18</sub> reverse phase column (Waters). The column was preconditioned prior to sample loading by washing once with 100% methanol and five times thereafter with 0.1% (v/v) TFA (trifluoroacetic acid). After the sample had passed through the column, salts were removed by washing with 0.1% TFA for five column volumes. This was followed by elution with 100% methanol, and the collected orange fractions were evaporated overnight at room temperature. The collected product (6 mg) was identified as (H<sub>2</sub>O)OHcbi by its UV–visible absorption spectrum, which was identical to the spectrum reported in the literature.<sup>35,36</sup>

## RESULTS AND DISCUSSION

**Overproduction, Reconstitution, and Specific Activities.** 3–5 mg of MBP-tagged VcrA-MBP was produced from 3 g of cells (wet weight). VcrA, as isolated from *Dehalococcoides mccartyi* strain VS, was shown previously to contain molar ratios of Fe and S consistent with a stoichiometry of two [4Fe–4S] clusters as well as one corrinoid cofactor per enzyme; the monomeric enzyme is membrane-associated putatively via a small integral membrane protein (VcrB) facing the outside<sup>10,16</sup> (see Supporting Information Figure S1). Heterologous overproduction of VcrA-MBP from plasmid pLIC-HMK resulted in the formation of inclusion bodies, and all VcrA-MBP was found

in the insoluble fraction (data not shown). No significant soluble VcrA-MBP was observed upon increasing the induction time beyond 3 h, or by varying the growth medium between several rich (LB, Standard I, TB) or minimal media containing glucose, the growth temperatures from 16 to 37 °C, the host *E. coli* strain (BL21, BL21 DE3, BL21pLys) or the inducer concentration between 50 and 1000  $\mu\text{M}$  (data not shown). Therefore, VcrA-MBP was purified from inclusion bodies under denaturing conditions to apparent homogeneity using His-tag affinity chromatography. Using a Ni-IDA matrix column, nearly homogeneous protein was obtained (Figure 1). Subsequently, the denatured protein was desalted in the presence of 20% glycerol and 0.2% CHAPS followed by refolding and reconstitution of the cobalamin and iron–sulfur cluster cofactors. Excess cofactors were removed, and metal analysis (via ICP-MS and spectrophotometric estimation) was performed, indicating a 1–1.4 mol Co and 8–12 mol nonheme iron ratio per mol purified VcrA-MBP. When reconstituted VcrA was subjected to the same analysis, a Co content of 0.8–1.1 mol and a nonheme iron content of 7–10 mol per mol of purified enzyme were found.

Heterologously produced and cofactor-reconstituted VcrA-MBP catalyzed the reduction of vinyl chloride, 1,1-DCE, *cis*- and *trans*-1,2-DCE at high specific activities (Table 1). Vinyl chloride was reductively dehalogenated to ethene at a  $V_{\max}$  of 1050  $\text{nmol min}^{-1} [\text{mg protein}]^{-1}$  and a  $K_M$  of 10  $\mu\text{M}$ , which is very similar to the specific activity of the purified, native VcrA (990  $\text{nmol min}^{-1} [\text{mg protein}]^{-1}$ ), for which a  $K_M$  was not reported.<sup>10</sup> Also, 1,1-DCE was dehalogenated to vinyl chloride and ethene at a  $V_{\max}$  of about 295  $\text{nmol min}^{-1} [\text{mg protein}]^{-1}$  ( $K_M = 50 \mu\text{M}$ ) (Table 1, Figure 2a). 1,1-DCE undergoes a two-step conversion into ethene via vinyl chloride as intermediate and does not follow Michaelis–Menten behavior below 10  $\mu\text{M}$  (data not shown). 1,1-DCE in native VcrA proceeded at a  $V_{\max}$  of 390  $\text{nmol min}^{-1} [\text{mg protein}]^{-1}$ .<sup>10</sup> When testing as an abiotic control coenzyme B<sub>12</sub> at equivalent molar concentration but without VcrA in the assay, a slow rate of vinyl chloride reduction of 100 nmol/min was observed (data not shown). For 1,1-DCE dehalogenation, the maximum abiotic dechlorination rates were about 25 nmol/min, which is less than 10% of the enzymatic rate, at B<sub>12</sub> concentrations comparable to those present in the enzyme.

Interestingly, VcrA-MBP was also found to mediate the dihaloelimination of 1,2-DCA to ethene (Table 1; Figure 2b). This is a novel activity and was not previously observed. The maximum specific activity of complete 1,2-DCA dehalogenation by VcrA-MBP was 450  $\text{nmol min}^{-1} [\text{mg protein}]^{-1}$  (Table 1). However, the  $K_M$  of 1300  $\mu\text{M}$  is 2 orders of magnitude higher than that for vinyl chloride or 1,1-DCE, suggesting that 1,2-DCA may not be a physiological substrate in situ for VcrA. This extended substrate specificity of VcrA has implications for chlorinated solvent-contaminated sites, which contain both

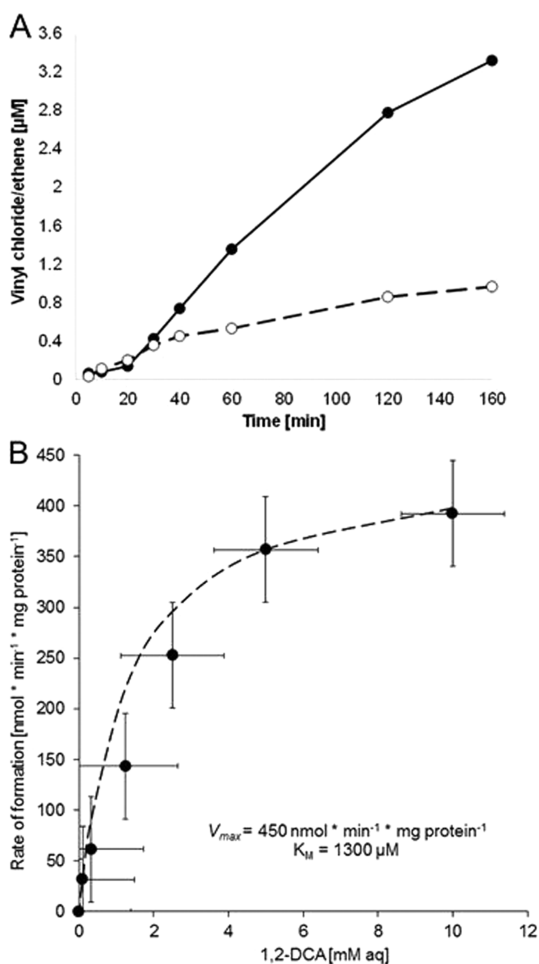


**Figure 2.** (A) Reduction of 1,1-DCE to vinyl chloride (VC, O) and ethene (Et, ●) by VcrA-MBP. The curve fitting suggests that the formation of both products follows second-order kinetics. (B) Kinetics of 1,2-DCA dihaloelimination to ethene by VcrA-MBP. The Michaelis–Menten parameters were estimated as  $K_M = 1300 \text{ } \mu\text{M}$  and  $V_{max} = 450 \text{ nmol min}^{-1} [\text{mg protein}]^{-1}$ . The “●” are the measured data points, while the dotted line represents the simulation based on the Michaelis–Menten equation. The cross-marks represent error bars.

chloroethanes and chloroethenes. *Dehalococcoides* VS could be expected to consume 1,2-DCA faster than vinyl chloride, 1,1- or the 1,2-DCE isomers, but only if the initial concentration of the former is much higher than those of the chloroethenes and higher than those encountered in most natural environments. It is unclear whether 1,2-DCA dihaloelimination is also coupled to energy conservation in vivo. However, 1,2-DCA is also far more water-soluble (up to 100 mM) than the chloroethenes, so the actual dechlorination rates in the environment may be different from what the Michaelis–Menten parameters predict.

**Methyl Viologen-Independent Dehalogenation.** Consistent with previous in vitro dehalogenation studies,<sup>37,38</sup> the presence of methyl viologen for reductive dehalogenation activity of VcrA-MBP was not essential, although a methyl viologen-induced acceleration of the reaction rates was observed. Methyl viologen-independent dehalogenation rates in this case were about 20–25% of the rates in the presence of methyl viologen (Table 1).

Interestingly, upon removal of the MBP tag via proteolytic cleavage, the purified and cofactor-reconstituted VcrA also showed dehalogenation activity regardless of whether methyl

viologen was absent or present. The methyl viologen-independent rates were 45–55% of the rates observed in the presence of methyl viologen (Table 1). The fact that methyl viologen accelerates the rates of dechlorination both in VcrA-MBP and in VcrA suggests that it could create a chemical shortcut for transferring electrons directly onto Co(II) to form the catalytically active Co(I) species, but the actual rates further depend on steric factors based on the conformation of the enzyme.

**EPR Studies.** X-band CW EPR spectra of VcrA-MBP and VcrA were recorded under different reducing conditions. In the presence of 2 mM 2-mercaptoethanol, the observed EPR spectrum (top trace) of VcrA-MBP was nearly axial with  $g$ -values = [2.29, 2.23, 2.004] (blue trace, Figure 3A). The octet centered about  $g_{\parallel} = 2.004$  results from the splitting of the resonance due to the hyperfine interaction of the unpaired electron with the  $I = 7/2$   $^{59}\text{Co}$  nucleus (100% natural abundance);  $A_{\parallel}(^{59}\text{Co}) = 305 \text{ MHz}$ . Each of these lines was further split into a triplet due to an additional hyperfine interaction with a single  $I = 1$   $^{14}\text{N}$  nucleus ( $A_{\parallel}(^{14}\text{N}) = 52 \text{ MHz}$ ). These EPR spectral features are consistent with their assignment to a Cob(II)alamin species for which either the pendant dimethylbenzimidazole (DMB) is bound axially to the cobalt center or this DMB base has been replaced by some other nitrogenous ligand such as a histidine side chain from the polypeptide.

The CW EPR spectra of VcrA-MBP reconstituted with either aquahydroxocobinamide or dicyanocobinamide are essentially identical to one another, but markedly different from the spectrum of the cobalamin-reconstituted enzyme (Supporting Information Figure S4). The  $g$ -values move slightly upfield and the  $^{14}\text{N}$  ligand hyperfine is lost when the enzyme is reconstituted with cobinamide instead of cobalamin. This indicates that the dimethylbenzimidazole base of the cobalamin is likely serving as a ligand to the VcrA-bound cofactor, not a proteinaceous histidine ligand as in methionine synthase. Recent studies showed that dimethylbenzimidazole was essential for *D. mccartyi* dehalogenation,<sup>39</sup> unlike in *Sulfurospirillum*-type microorganisms where the lower ligand is an adenine derivative. Therefore, our use of a dimethylbenzimidazole-containing corrinoid is relevant.

Further treatment of VcrA-MBP with the strong reductant Ti(III)-citrate left the Cob(II)alamin signal unchanged; however, a new intense signal appeared at  $g = [1.969, 1.928, 1.852]$  in the low-temperature EPR spectrum (Figure 3A, green trace). This new signal relaxed too quickly to be observed at temperatures above 60 K (Supporting Information Figure S5), which is consistent with the behavior of reduced [4Fe–4S] clusters. Integration of the individual EPR signals revealed that approximately 69% of the total signal corresponded to reduced [4Fe–4S] centers and 31% of the EPR spectrum corresponded to Cob(II)alamin, in line with the elemental analysis showing 1–1.4 Co mol and 8–12 mol nonheme iron per mol of enzyme (Supporting Information Table S1).

An additional signal appeared at  $g = [1.989, 1.928, 1.900]$  that varied in intensity with each preparation (Figure 3B). This new signal was greatly diminished following an additional rapid desalting step (via a 10 kDa cutoff Centricon membrane filter) in the sample preparation (Supporting Information Figure S6) and looked similar to signals measured recently for Ti(III)-containing compounds.<sup>40</sup> Thus, we concluded that the features at [1.989, 1.928, 1.900] arise from  $S = 1/2$  Ti(III) species generated during the reduction.

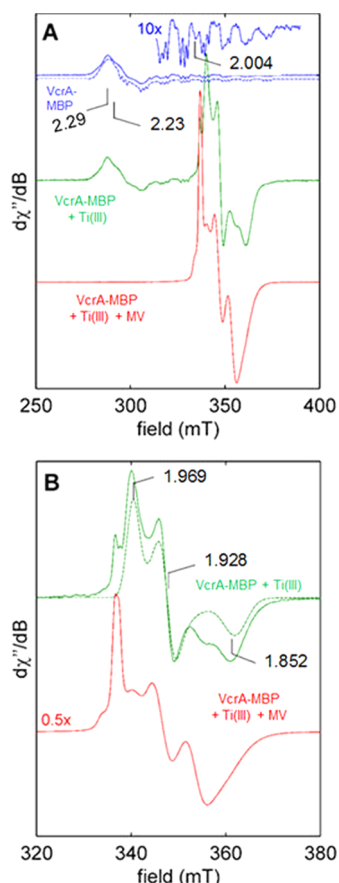


**Figure 3.** (A) X band (9.367 GHz) EPR spectra of VcrA-MBP at 15 K under different reducing conditions. (Top) 2-Mercaptoethanol-reduced VcrA-MBP (solid blue trace) with corresponding simulation (dashed blue trace) along with 10-fold magnification of features centered at  $g = 2.00$  to better illustrate the  $^{14}\text{N}$  hyperfine splitting. Ti(III)-reduced VcrA-MBP (middle, green trace) and Ti(III)-reduced VcrA-MBP following addition of methylviologen (bottom, red trace) are also shown. The  $g$ -values are indicated in the figure. Simulation parameters for the Cob(II)alamin species are as follows:  $g = [2.29, 2.23, 2.004]$ ;  $g$ -strain =  $[0.05, 0.04, 0.002]$ ;  $A(^{59}\text{Co}) = [50, 40, 305]$  MHz;  $A(^{14}\text{N}) = [5, 5, 52]$  MHz. Spin quantification of the difference spectrum from the green and blue traces showed that the FeS signals:cob(II)alamin ratio is approximately 2:1 (77:34) (see Supporting Information Table S1). (B) Expansion of EPR spectrum of Ti(III)-reduced VcrA-MBP (top, solid green trace) and corresponding simulation of the  $[4\text{Fe}-4\text{S}]^+$  contribution (dotted green trace) as compared to the spectrum of Ti(III)-reduced VcrA-MBP following addition of methylviologen (red trace). Simulation parameters for the  $[4\text{Fe}-4\text{S}]^+$  species are as follows:  $g = [1.969, 1.928, 1.851]$ ;  $g$ -strain =  $[0.017, 0.018, 0.028]$ .

Interestingly, although Ti(III)citrate should be a sufficiently strong reductant to reduce Cob(II)alamin to  $\text{Co}^{1+}$ , it seems insufficient to do so for cobalamin bound to VcrA-MBP. Only upon further addition of methyl viologen did the Cob(II)alamin EPR spectrum disappear. The intensity of the  $[4\text{Fe}-4\text{S}]^+$  signal was unchanged (Figure 3B). This spectral change coincided with the appearance of new features at  $\sim 385$  and  $\sim 555$  nm in the electronic absorption spectrum that is indicative of Cob(I)-alamin. Samples of Ti(III)-citrate and methyl viologen reduced VcrA with 1,1-DCE as a substrate or with 50  $\mu\text{M}$  iodoacetamide as an inhibitor did not change the spectra substantially (data not shown). The EPR spectra of the Ti(III)-reduced, cobalamin-reconstituted VcrA are similar to those of VcrA-MBP. Specifically, we observe signals from Co(II)Cbl (not shown) as

well as signals from two reduced  $[4\text{Fe}4\text{S}]$  clusters and adventitious Ti(III) species (Supporting Information Figure S7). Both FeS cluster signals observed in samples of VcrA lacking the MBP tag possess slightly different  $g$ -tensors than that determined for the FeS cluster in the samples of VcrA-MBP. The origin of these differences is unclear at this time. However, subtle changes in  $g$ -values are expected if the MBP tag influences the structure of VcrA. Second-coordination sphere interactions are well-known to modulate EPR properties of FeS clusters. Additionally, it is possible that in these samples both clusters in VcrA (two  $[4\text{Fe}-4\text{S}]$  clusters being suggested by iron content analysis) are reduced and in sufficiently close proximity to one another so as to cause a shifting of some of the resonant field positions due to through-space spin-dipole interactions. This hypothesis will be evaluated in the future using multifrequency EPR techniques.

The intensity of the Cob(II)alamin signal was reduced by approximately 70% upon oxidation by the presence of 10 mM ferricyanide (Figure 4). Upon addition of up to 50–75 mM

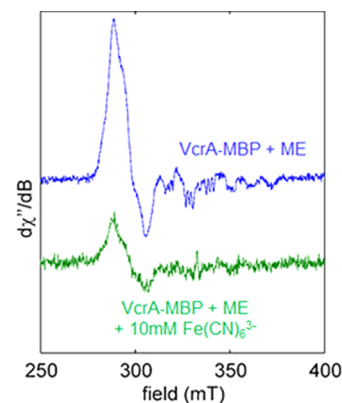


**Figure 4.** Chemical oxidation in the absence of oxygen of 2-mercaptoethanol reduced VcrA-MBP: The top trace shows the X-band EPR spectrum VcrA-MBP reduced with 2-mercaptoethanol, whereas the bottom trace shows the same sample treated with 10 mM ferricyanide. The intensity of the Cob(II)alamin signal is reduced by about 70%; upon the further addition of ferricyanide (50–75 mM), the signal is completely abolished (data not shown). No  $[3\text{Fe}-4\text{S}]$  signals were observed.

ferricyanide, the Co(II) signal was completely abolished (data not shown), and no new signals appeared except for a broad derivative feature that was also present in spectra of samples containing only 1 mM ferricyanide. Chemical oxidation in the absence of molecular oxygen yielded oxidized  $[4\text{Fe}-4\text{S}]$  cluster(s) and oxidized cobalamin that are both EPR silent. No EPR evidence for oxidized  $[3\text{Fe}-4\text{S}]$  clusters was found in the ferricyanide-treated samples.<sup>41</sup>

**UV-Visible Spectrophotometry.** Titration of VcrA-MBP with Ti(III)-citrate up to concentrations of 1.6 mM reduced the intensities of the iron-sulfur signal (420 nm) and produced peaks at 385 and 475 nm (Supporting Information Figure S8, panel A). Estimation of the Cob(I)alamin versus Cob(II)alamin using the reported extinction coefficients (see methods section) showed only about 10% of the cobalamin in the Co(I) state. However, if 0.4 mM methyl viologen was added to VcrA-MBP, then the sequential titration with Ti(III)-citrate produced increasing absorption of three sharp peaks at 366 nm, 385 nm, characteristic of the Co(I) state (Supporting Information Figure S8, panel B), and 395 nm. A broad peak also appeared for

reduced methyl viologen at 600 nm, and the intensity of the peak for Co(I) around 555 nm increased (Supporting Information Figure S8, panel B). The spectrum of free methyl viologen and Ti(III)-citrate overlaps considerably with that of VcrA-MBP reduced with methyl viologen and Ti(III)-citrate from 350 to 450 nm, and is quite different from that of the unreduced enzyme (Supporting Information Figure S8, panel C). Further, Cob(I)-alamin also spontaneously reoxidizes to the Co(II) state. This makes the accurate quantification of Cob(I)- versus Cob(II)-alamins in the methyl viologen-reduced enzyme difficult. However, VcrA-MBP undergoes a shift of a peak from 530 nm for Co(II) to 555 nm typical for Co(I) upon reduction; we estimated about 70–90% of the cobalamin must be in the Co(I) state based on the absorption at 555 nm (calculated extinction  $9.0 \text{ mM}^{-1} \text{ cm}^{-1}$ ).

In contrast, VcrA (lacking MBP) exhibited quite different UV–vis spectroscopic features upon reduction by Ti(III)-citrate (Supporting Information Figure S9, panel A). An intense peak at 388 nm characteristic of Cob(I)alamin and a smaller peak at 550 nm appeared for 1 mM Ti(III) in the absence of methyl viologen. Concomitant with the appearance of the Cob(I)alamin signal, the 475 nm Cob(II)alamin maximum was replaced by another at 465 nm (which shows that cobalamin is still bound to VcrA). The spectra measured in this experiment are strikingly similar to those of the corrinoid iron sulfur protein<sup>42</sup> where Co(I)corrinoid species also play a key catalytic role.

On the basis of the extinction coefficients estimated in our study, we calculated that about 99% of the enzyme-bound cobalamin was reduced to the Co(I) state at approximately 1.5 mM of Ti(III). The methyl viologen-mediated spectra of VcrA were similar to those of VcrA-MBP with methyl viologen (Supporting Information Figure S9, panel B). The disappearance of the Co(II)Cbl signal as assessed by EPR spectroscopy is correlated to the appearance Co(I)Cbl features in the UV–visible spectrum, demonstrating the presence of Co(I)Cbl in the catalytically competent form of VcrA.

## CONCLUSIONS

We have established a heterologous platform to produce the VcrA enzyme, which can be reconstituted in the fully active form. This is also the first biochemical report to unambiguously demonstrate the existence of a bifunctional chloroethene and chloroethane reductive dehalogenase. This observation has strong implications for the remediation of sites cocontaminated with chloroethenes and chloroethanes.

Interestingly, although the exact chemical identity of the corrinoid cofactor of native VcrA is unknown, heterologously expressed VcrA-MBP reconstituted with hydroxocobalamin or adenosylcobalamin has kinetic properties that are indistinguishable from that of native VcrA. Because we did not use dark/red light conditions, the active species was likely to be hydroxocobalamin. The use of either cobalamin derivative did not lead to any difference in the specific activity (data not shown). On the basis of the findings reported here, we propose that native VcrA coordinates Cob(II)alamin with an  $^{14}\text{N}$  axial ligand, which arises most likely from the dimethylbenzimidazole moiety of the cofactor. Earlier corrinoid cross-feeding studies<sup>8</sup> suggested that dimethylbenzimidazole (DMB), the lower ligand of cobalamins, was essential for the reductive dechlorination of chloroethenes by defined microbial consortia containing *D. mccartyi*, which is consistent with our findings. Base-on cobalamins were reported to have Co(II)/Co(I) reduction potentials of about  $-600 \text{ mV}$  (SHE), while base-off cobalamins

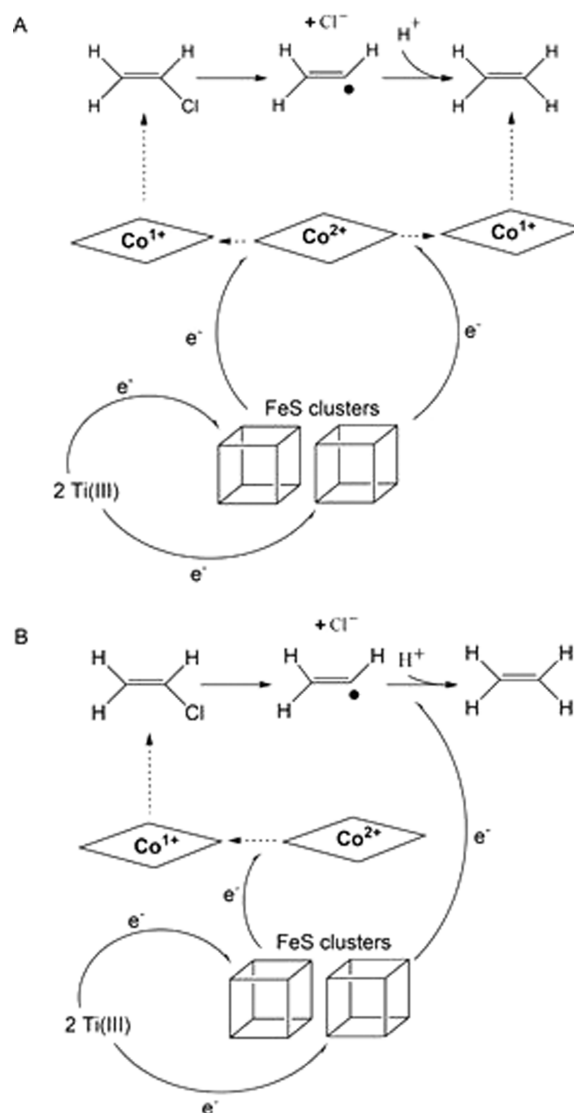


**Figure 5.** Proposed reaction mechanism(s) for reductive dehalogenation by VcrA; Co(II) is reduced to Co(I) by a low potential ferredoxin/ flavodoxin physiologically or Ti(III) in vitro. Co(I) donates an electron to the substrate eliminating Cl<sup>-</sup> and generating a substrate radical; this radical is further reduced by an electron originating either from a second Co(I) as in (A) or directly by a [4Fe–4S] cluster as in (B); protonation possibly simultaneous to the second reduction leads to the formation of the product. Vinyl chloride is shown as the substrate here, but the same mechanism could dechlorinate 1,1-DCE and other substrates.

potentials are around  $-500 \text{ mV}$ .<sup>43</sup> The exact potential of the Co(II)/Co(I) couple depends on the interaction of the cobalamin with the polypeptide. The [4Fe–4S] clusters that are reducible by Ti(III) in vitro may be reduced in vivo possibly by ferredoxin/ flavodoxin. We can distinguish only one class of EPR signals associated with the reduced [4Fe–4S] clusters. Thus, the two putative clusters are either spectroscopically equivalent or we are only able to observe one of two classes under our experimental conditions. Furthermore, these clusters do not necessarily have different reduction potentials. A chemical model study of the dehalogenation of chloroethenes reported a reduction potential in free solution of  $-450 \text{ mV}$  for the vinyl radical with much more positive potentials for the chloroethyl radicals.<sup>44</sup> Thus, a mechanism where a Cob(I)alamin species donates an electron to the chlorinated compound, leading to

radical dechlorination (Figure 5), may be envisaged. The vinyl-type radical could be finally reduced by either a [4Fe–4S] cluster (as in Figure 5B) or a second Co(I) (as in Figure 5A) and protonated to yield the product.

A nucleophilic mechanism has also been suggested in recent work on the crystal structures of PCE dehalogenase<sup>45</sup> and of NpRdhA.<sup>18</sup> The mechanism is similar to that proposed by Ragsdale and others for the dehalogenation of 3-chloro-4-hydroxy benzoic acid.<sup>46</sup> However, if geometric constraints prevent a direct nucleophilic attack by Co(I) on the substrate carbon bearing the halide in VcrA, an alternative mechanism involving direct interaction of Co(I) with the halogen would be plausible, as has been proposed for NpRdhA.<sup>18</sup> While the proposed mechanism serves as a basis for future experiments with recombinant VcrA, our studies reported here provided novel insights into an environmentally important *Dehalococcoides*-type reductive dehalogenase.

## ■ ASSOCIATED CONTENT

### Supporting Information

Figures S1–S9 and Table S1. This material is available free of charge via the Internet at <http://pubs.acs.org>.

## ■ AUTHOR INFORMATION

### Corresponding Author

\*spormann@stanford.edu

### Notes

The authors declare no competing financial interest.

## ■ ACKNOWLEDGMENTS

Funding for this work was provided by ENI and NSF to A.M.S. and by the National Institutes of Health to (GM-104543) R.D.B. We thank Dick Winant (PMF at the PAN Center, Stanford), Guangchao Li (ICP-MS at the School of Earth Sciences, Stanford), and Koshlan Meyer-Blackwell and Maeva Fincker for helpful discussions. We thank Maeva Fincker also for critically reading the manuscript and useful comments.

## ■ REFERENCES

- (1) Squillace, P. J.; Moran, M. J.; Lapham, W.; Price, C.; Clawges, R.; Zogorski, J. S. *J. Environ. Sci. Technol.* **1999**, *33*, 4176.
- (2) Sutfin, J. A. *Int. Groundwater Technol.* **1996**, *2*, 7.
- (3) US EPA, T. I. O. Bioremediation of chlorinated solvent contaminated groundwater, 1998.
- (4) Golding, B. T.; Anderson, R. A.; Ashwell, S.; Edwards, C. H.; Garnett, I.; Kroll, F.; Buckel, W. In *Vitamin B12 and B12 Proteins*; Kräutler, B., Arigoni, D., Golding, B. T., Eds.; Wiley-VCH: Weinheim, 1998; p 209.
- (5) Sjuts, H.; Fisher, K.; Dunstan, M. S.; Rigby, S. E.; Leys, D. *Protein Expression Purif.* **2012**, *85*, 224.
- (6) Schmitz, R. P. H.; Habel, A.; Ploss, K.; Boland, W.; Wolf, J.; Neumann, A.; Svatos, A.; Diekert, G. *Environ. Sci. Technol.* **2007**, *41*, 7370.
- (7) van de Pas, B. A.; Smidt, H.; Hagen, W. R.; van der Oost, J.; Schraa, G.; Stams, A. J. M.; de Vos, W. M. *J. Biol. Chem.* **1999**, *274*, 20287.
- (8) van de Pas, B. A.; Gerritse, J.; de Vos, W. M.; Schraa, G.; Stams, A. J. M. *Arch. Microbiol.* **2001**, *176*, 165.
- (9) Magnuson, J. K.; Romine, M. F.; Burris, D. R.; Kingsley, M. T. *Appl. Environ. Microbiol.* **2000**, *66*, 5141.
- (10) Müller, J. A.; Rosner, B. M.; von Abendroth, G.; Meshulam-Simon, G.; McCarty, P. L.; Spormann, A. M. *Appl. Environ. Microbiol.* **2004**, *70*, 4880.
- (11) Grostern, A.; Edwards, E. A. *Appl. Environ. Microbiol.* **2009**, *75*, 2684.

- (12) Marzorati, M.; Balloi, A.; de Ferra, F.; Corallo, L.; Carpani, G.; Wittebolle, L.; Verstraete, W.; Daffonchio, D. *Microb. Cell Fact.* **2010**, *9*, 1.
- (13) Schumacher, W.; Holliger, C. *J. Bacteriol.* **1996**, *178*, 2328.
- (14) Louie, T. M.; Mohn, W. W. *J. Bacteriol.* **1999**, *181*, 40.
- (15) Miller, E.; Wohlfarth, G.; Diekert, G. *Arch. Microbiol.* **1996**, *166*, 379.
- (16) Rosner, B. M.; Spormann, A. M.; McCarty, P. L. *Appl. Environ. Microbiol.* **1997**, *63*, 4139.
- (17) Mac Nelly, A.; Kai, M.; Svatoš, A.; Diekert, G.; Schubert, T. *Appl. Environ. Microbiol.* **2014**, *80*, 4313.
- (18) Payne, K. A. P.; Quezada, C. P.; Fisher, K.; Dunstan, M. S.; Collins, F. A.; Sjuts, H.; Levy, C.; Hay, S.; Rigby, S. E. J.; Leys, D. *Nature* **2014**, published online.
- (19) Sambrook, J.; Maniatis, T.; Fritsch, E. F. *Molecular Cloning: A Laboratory Manual*; Cold Spring Harbor Laboratory: New York, 1989; Vols. 1 and 2.
- (20) Doyle, S. A. *Methods Mol. Biol.* **2005**, *310*, 107.
- (21) Kapust, R. B.; Waugh, D. S. *Protein Sci.* **1999**, *8*, 1668.
- (22) Corn, J. E.; Pease, P. J.; Hura, G. L.; Berger, J. M. *Mol. Cell* **2005**, *20*, 391.
- (23) Studier, F. W. *Protein Expression Purif.* **2005**, *41*, 207.
- (24) Anspach, F. B. *J. Chromatogr., A* **1994**, *672*, 35.
- (25) Hemdan, E. S.; Porath, J. *J. Chromatogr.* **1985**, *323*, 255.
- (26) Smith, F. E.; Herbert, J.; Gaudin, J.; Hennessy, D. J.; Reid, G. R. *Clin. Biochem.* **1984**, *17*, 306.
- (27) Fish, W. W. *Methods Enzymol.* **1988**, *158*, 357.
- (28) Baker, S. A.; Miller-Ihli, N. J. *Spectrochim. Acta, Part B* **2000**, *55*, 1823.
- (29) Chen, J. H.; Jiang, S. J. *J. Agric. Food Chem.* **2008**, *56*, 1210.
- (30) Freedman, D. L.; Danko, A. S.; Verce, M. F. *Water Sci. Technol.* **2001**, *43*, 333.
- (31) Bechtel, J. T.; Winant, R. C.; Ganem, D. *J. Virol.* **2005**, *79*, 4952.
- (32) Stoll, S.; Schweiger, A. *J. Magn. Reson.* **2006**, *178*, 42.
- (33) Eaton, G. R.; Eaton, S. S.; Quine, R. W.; Mitchell, D.; Kathirvelu, V.; Weber, R. T. *J. Magn. Reson.* **2010**, *205*, 109.
- (34) Goulding, C. W.; Postigo, D.; Matthews, R. G. *Biochemistry* **1997**, *36*, 8082.
- (35) Brodie, J. D. *Proc. Natl. Acad. Sci. U.S.A.* **1969**, *62*, 461.
- (36) Blackledge, W. C.; Blackledge, C. W.; Griesel, A.; Mahon, S. B.; Brenner, M.; Pilz, R. B.; Boss, G. R. *Anal. Chem.* **2010**, *82*, 4216.
- (37) Neumann, A.; Siebert, A.; Trescher, T.; Reinhardt, S.; Wohlfarth, G.; Diekert, G. *Arch. Microbiol.* **2002**, *177*, 420.
- (38) Nijenhuis, I.; Zinder, S. H. *Appl. Environ. Microbiol.* **2005**, *71*, 1664.
- (39) Men, Y.; Seth, E. C.; Yi, S.; Allen, R. H.; Taga, M. E.; Alvarez-Cohen, L. *Appl. Environ. Microbiol.* **2014**, *80*, 2133.
- (40) Maurelli, S.; Morra, E.; Van Doorslaer, S.; Busico, V.; Chiesa, M. *Phys. Chem. Chem. Phys.* **2014**, *16*, 19625.
- (41) Liu, A.; Gräslund, A. *J. Biol. Chem.* **2000**, *275*, 12367.
- (42) Kung, Y.; Ando, N.; Doukov, T. I.; Blasiak, L. C.; Bender, G.; Seravalli, J.; Ragsdale, S. W.; Drennan, C. L. *Nature* **2012**, *484*, 265.
- (43) Banerjee, R. V.; Harder, S. R.; Ragsdale, S. W.; Matthews, R. G. *Biochemistry* **1990**, *29*, 1129.
- (44) Pratt, D. A.; van der Donk, W. A. *J. Am. Chem. Soc.* **2005**, *127*, 384.
- (45) Bommer, M.; Kunze, C.; Fesseler, J.; Schubert, T.; Diekert, G.; Dobbek, H. *Science* **2014**, *346*, 455.
- (46) Krasotkina, J.; Walters, T.; Maruya, K. A.; Ragsdale, S. W. *J. Biol. Chem.* **2001**, *276*, 40991.

## ■ NOTE ADDED AFTER ASAP PUBLICATION

The last paragraph of the Conclusion section has been revised in the version of this paper published March 4, 2015. The corrected version published March 5, 2015.